NJC

Structural characterization of naphthalene sulfonamides and a sulfonate ester and their in vitro efficacy against *Leishmania tarentolae* promastigotes

Journal:	*New Journal of Chemistry*
Manuscript ID	NJ-ART-12-2020-006320.R1
Article Type:	Paper
Date Submitted by the Author:	08-Feb-2021
Complete List of Authors:	Li, Edward; Illinois State University, Department of Chemistry; William Fremd High School Katinas, Jade; Illinois State University, Department of Chemistry Jones, Marjorie; Illinois State University, Chemistry; Hamaker, Christopher; Illinois State University, Department of Chemistry

ARTICLE

Structural characterization of naphthalene sulfonamides and a sulfonate ester and their *in vitro* efficacy against *Leishmania tarentolae* promastigotes

Received 00th January 20xx,
Accepted 00th January 20xx

DOI: 10.1039/x0xx00000x

Edward W. Li[a,b], Jade Katinas[a], Marjorie A. Jones[a], and Christopher G. Hamaker[a,*]

Leishmaniasis, a parasitic infectious disease transmitted by sandfly bites, is an extremely complex human and veterinary disease. In humans, it takes different forms ranging from self-healing cutaneous ulcers to severe, life-threatening visceral infections. Current treatments primarily rely on chemotherapies. The current chemotherapeutic drugs, developed decades ago, are costly, toxic, and have become problematic due to drug resistance. To this end, two naphthalene sulfonamides and one naphthalene sulfonate ester were subjected to a structure-activity relationship (SAR) study for inhibition of *Leishmania*. The new chlorosulfonamide, *N*-(2'-chlorophenyl)-1-naphthalene sulfonamide (**B**), and sulfonate ester, 3-methyl-4-((naphthalen-1-ylsulfonyl)oxy)benzoic acid achieved (**C**) IC_{50} values of 9.5 µM and 7.4 µM, respectively, against *Leishmania tarentolae* promastigotes in vitro, which are notably lower than the IC_{50} value of 49 µM for our benchmark compound, *N*-(4'-carboxy-2'-methylphenyl)-1-napthalenesulfonamide (**A**). Additionally, all three compounds were analyzed by X-ray crystallography and show strong intermolecular interactions in the crystalline state. The new findings from this SAR study open new directions for advanced leishmaniasis treatment.

Introduction

Leishmaniasis is an extremely complex human and veterinary disease, transmitted by sandfly bites.[1] In humans, the disease takes different forms ranging from self-healing cutaneous ulcers to a severe life-threatening infection.[1] According to the World Health Organization, leishmaniasis is endemic in 95 countries, from rain forests in Central and South America to deserts in the Middle East and West.[2] Some cases of the disease have also appeared in Mexico and Texas.[2] The disease not only affects people who live in countries where the disease is endemic but also poses a risk to people who travel in those areas.[2] For example, the cutaneous form of the disease is a growing health problem for U.S. military service members in sandfly-rich Afghanistan and Iraq.[2] First line treatments for leishmaniasis rely on pentavalent antimonials and amphotericin B, both of which are toxic to humans, and many strains of *Leishmania* are gaining resistance to these oft-used drugs.[3-8] To combat this emerging global health threat, there is urgent need for new anti-leishmanial drug development.

Sulfonamides, known as sulfa drugs, have been used as treatments against bacterial infections and are also of interest in treating leishmaniasis.[9,10] In previous work, Peixoto and Beverley studied the effects of sulfonamides and sulfones against *Leishmania major* promastigotes *in vitro*. Some of their sulfonamides and a sulfone were found to be inhibitory against the parasite, though with rather high IC_{50} values, over 150 µM.[11] Since then, interest in sulfonamides and sulfones has grown for treatment against leishmaniasis; however previous candidates failed as a treatment solution.[8,12-16] Metal dithiocarbamates have also been recently examined for their anti-leishmanial activity.[17] Recently, we reported a new class of naphthalene sulfonamides (**Figure 1**, General Structure Z = NH) which gave promising in vitro anti- leishmanial properties.[18] It was found that the ortho and para substituents, X and Y, play an important role in the sulfonamides' leishmanicidal activities, water solubilities, and a possible mechanism of action.[18] In compounds with X = -CH_3 and Y = H, the sulfonamides have superior activities relative to those with X = H, -OCH_3, or -SCH_3, in spite of poor solubility. When Y is a carboxylic acid group, the methyl

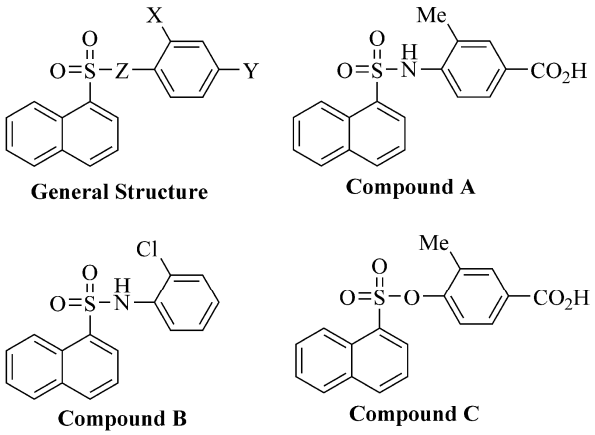

Figure 1. General Structure and structures of compounds **A**, **B**, and **C**.

[a] Department of Chemistry, Illinois State University, Normal, IL 61790-4160
[b] William Fremd High School, Palatine, IL
Electronic Supplementary Information (ESI) available: [details of any supplementary information available should be included here]. See DOI: 10.1039/x0xx00000x

sulfonamide solubility issue was greatly improved, but inhibitory activity was reduced. These interesting results led us to speculate that the size of X (larger than X = H but smaller than X = OCH_3) and the polarity of X will affect inhibitory activity and may bring new insight into the structure-activity relationship (SAR). Looking beyond traditional sulfonamides and sulfones for new chemistry at the Z position was another inspiration for this anti-leishmanial study.

Encouraged by our previous results, and the fact that *L. tarentolae* has been shown to be a very useful model for screening antileishmanial agents,[19] we have designed a novel naphthalene halogenated sulfonamide and a naphthalene sulfonate ester for the preliminary screening against *L. tarentolae* for this SAR study. To this end, the new compounds (**Figure 1**), chlorosulfonamide **B** and sulfonate ester **C**, were synthesized. Both compounds **B** and **C** resulted in remarkable inhibition against L. tarentolae promastigotes compared to the benchmark naphthalene sulfonamide **A** reported previously.[18]

Experimental

Reagents and materials were purchased from commercial sources and used directly unless stated otherwise. NMR spectra were obtained at 302 K in $CDCl_3$ or DMSO-*d*6 at a frequency of 500.13 MHz for ^{1}H and 125.76 MHz for ^{13}C spectra. Mass spectroscopy data were acquired using positive ion mode electrospray ionization on a high resolution time of flight mass spectrometer.

X-ray crystallography

Data for **B** were collected at 297(2) K on a Bruker-Nonius CAD4/Mach3 diffractometer using MoKα radiation (λ = 0.71073 Å). Data collection and cell refinement were performed using CAD4 express.[20] Data reduction was carried out using XCAD4.[21] Unit cell parameters were obtained from a least-squares refinement of 25 centered reflections. The data were corrected for absorption through use of empirical psi-scans.[22] Data for **A** and **C** were collected on a Bruker APEX II CCD diffractometer at 100(2) K using MoKα radiation (λ = 0.71073 Å). The data were processed using the Bruker SAINT software package and were corrected for absorption using SADABS. Structures were solved by direct methods using SHELXS-2017.[23] The data were refined using SHELXL-2017. All non-H atoms were refined anisotropically. Hydrogen atoms attached to carbon were assigned positions based on the geometries of their attached carbons. Hydrogen atoms bonded to oxygen and nitrogen were assigned positions based on the Fourier difference map. See **Table S1** for final refinement parameters.

Synthesis of compounds

***N*-(4'-carboxy-2'-methylphenyl)-1-napthalenesulfonamide**, **A**, was synthesized as previously reported.[18] Single crystals of **A** were grown by slow evaporation of an acetone solution of the compound. ^{1}H NMR (δ, ppm, DMSO-d6): 12.76 (br, 1H, COO*H*), 10.17 (s, 1H, N*H*), 8.73 (d, 1H, J_{HH} = 8.6 Hz), 8.22 (d, 1H, J_{HH} = 8.3 Hz), 8.08 (m, 2H,), 7.68 (m, 2H), 7.59 (m, 3H), 7.20 (d, 1H, J_{HH} = 8.2 Hz), 1.96 (s, 3H, C*H*$_3$). ^{13}C NMR (δ, ppm, dmso-d6): 166.71 (*C*OOH), 139.17, 135.12, 134.44, 133.79, 132.04, 131.71, 129.38, 129.07, 127.98, 127.60, 127.52, 127.38, 127.01, 124.46, 124.42, 123.67, 17.55 (*C*H$_3$). $C_{18}H_{15}NO_4S$, ESI-HRMS: m/z calc (found), intensity: $[M+H]^+$, 342.0800 (342.0784), 25%; $[M+Na]^+$, 364.0619 (364.0620), 100%; $[M+K]^+$, 380.0359 (380.0342), 20%.

***N*-(2'-chlorophenyl)-1-naphthalenesulfonamide** (**B**). To 20 mL of pyridine was added 2.266 g (10.00 mmol) 1-naphthalenesulfonyl chloride and 1.276 g (10.01 mmol) 2-chloroaniline. The mixture was refluxed for 30 minutes and then poured into 100 mL water to form a precipitate. The solid was filtered, washed with water, and dried to yield 2.052 g (64.6%) of compound **B** as a white solid. Single crystals of **B** were grown by slow evaporation of a 1,2-dichloroethane solution of **B**. ^{1}H NMR (δ, ppm, $CDCl_3$): 8.65 (dd, 1H, J_{HH} = 8.6, 0.8 Hz), 8.21 (dd, 1H, J_{HH} = 7.4, 1.2 Hz), 8.02 (d, 1H, J_{HH} = 8.3 Hz), 7.89 (dd, 1H, J_{HH} = 8.7, 0.6 Hz), 7.65 (m, 1H), 7.65 (m, 1H), 7.56 (m, 2H), 7.45 (t, 1H, J_{HH} = 8.1 Hz), 7.21 (br s, 1H, N*H*), 7.14 (m, 2H), 6.94 (m, 1H). ^{13}C NMR (δ, ppm, $CDCl_3$): 135.21, 134.48, 134.13, 133.78, 130.56, 129.57, 129.33, 128.73, 128.37, 127.97, 127.25, 125.66, 124.70, 124.48, 124.17, 121.61. $C_{16}H_{12}ClNO_2S$, ESI-HRMS: m/z calc (found), intensity: $[M+H]^+$, 318.0356 (318.0334), 60%; $[M+H]^+$, 320.0326 (320.0302), 23%; $[M+Na]^+$, 340.0175 (340.0152), 100%; $[M+Na]^+$, 342.0146 (342.0120), 35%; $[M+K]^+$, 355.9914 (355.9890), 20%; $[M+K]^+$, 357.9872 (357.9860), 8%.

3-Methyl-4-[(naphthalen-1-ylsulfonyl)oxy]benzoic acid (**C**). To a solution of 4-hydroxy-3-methylbenzoic acid (1.521 g, 10.00 mmol) in 10 mL 2*M* aqueous sodium hydroxide was added dropwise a solution of 2.266 g (10.00 mmol) 1-naphthalenesulfonyl chloride in 10 mL acetone. The mixture was allowed to stir at room temperature for 24 hours when approximately 2 mL of 6*M* aqueous hydrochloric acid was added to give a white precipitate. The precipitate was isolated by vacuum filtration, washed with dilute HCl and dried to yield 3.022 g (88.3%) of compound **C** as a white powder. Single crystals of **C** were grown by solvent diffusion of hexanes into a solution of **C** in acetone. ^{1}H NMR (δ, ppm, DMSO-d6): 8.66 (d, 1H, J_{HH} = 8.6 Hz), 8.44 (d, 1H, J_{HH} = 8.3 Hz), 8.20 (m, 2H), 7.87 (td, 1H, J_{HH} = 8.3, 1.0 Hz), 7.82 (br s, 1H, N*H*), 7.77 (t, 1H, J_{HH} = 7.6 Hz), 7.70 (t, 1H, J_{HH} = 7.8 Hz), 7.65 (dd, 1H, J_{HH} = 8.5, 1.7 Hz), 6.79 (d, 1H, J_{HH} = 8.5 Hz), 2.07 (s, 3H, C*H*$_3$). ^{13}C NMR (δ, ppm, dmso-d6): 166.49 (*C*OOH), 150.65, 133.86, 132.77, 131.06, 131.05, 130.60, 130.40, 129.46, 129.33, 128.48, 127.66, 127.54, 124.69, 123.99, 121.27, 15.87 (*C*H$_3$). 8.82 (dd, 1H), 8.18 (m, 2H), 8.01 (d, 1H), 7.91 (d, 1H), 7.77 (m, 1H), 7.74 (dd, 1H), 7.68 (m, 1H), 7.54 (t, 1H), 6.81 (d, 1H) $C_{18}H_{14}O_5S$, ESI-HRMS: m/z calc (found), intensity: $[M+H]^+$, 343.0641 (343.0625), 50%; $[M+Na]^+$, 365.0460 (365.0444), 100%; $[M+K]^+$, 381.0199 (381.0183), 15%.

Cell culture

For this study, all cell culture work was conducted in a sterile tissue culture hood under standard sterilized conditions. Following the method reported,[24] *L. tarentolae* promastigotes (ATCC strain 30143) were grown at room temperature (22° C) in Brain Heart Infusion (BHI) medium supplemented with 100 units Penicillin and 0.1 mg/mL Streptomycin (Sigma) and 10 μM hemin. To insure uniformity in the parasite quantity and age per

test cultures, *L. tarentolae* promastigotes were initially grown in 60 mL volumes (Falcon sterile culture flasks), and subsequently dispensed as uniform 5 or 10 mL aliquots into smaller (Falcon) sterile flasks for experimental testing following the method of Katinas *et al*.[18]

For each test, a control flask with cells was prepared using 1% (final volume) of dimethyl sulfoxide (DMSO) without any test compound additions. With addition of 1% DMSO alone, we found that cell viability is not affected significantly ($p > 0.05$) relative to cells not treated with DMSO. All inhibitors were prepared as 10 mM as stock solutions in DMSO and used to achieve the desired final concentration for each test. Care was taken to ensure that DMSO was added as needed to keep the final concentration consistently at 1%.

MTT viability assay and cell growth curve

MTT assay is a colorimetric assay that relies on the oxidoreductase enzymes in live cells to reduce the yellow MTT reagent (5mg/mL water) into the purple, insoluble formazan.[25] All assays were carried out in 96 well polypropylene microtiter plates (ThermoFisher) with 100 µL of the cell culture of interest per well followed by the addition of 10 µL of MTT reagent, then incubated for 1 hour following the method of Mosmann.[25] Absorbance values were recorded at 595 nm using the Bio-Rad iMark Microplate Reader. The corrected absorbance was calculated by subtracting the absorbance of a blank (BHI medium with 1% DMSO) from the absorbance of the sample of interest. For all studies, at least four replicates were performed at each data point and used to report the mean and standard deviation.

L. tarentolae promastigote growth curves with and without additions of test compounds, were determined by MTT assays at 24 hour intervals. Corrected A_{595nm} absorbance values, interpreted to reflect cell viability, are plotted as a function of cell culture age (days). Values are reported as the mean ± SD for n = 4 replicates.

Dose response and IC_{50}

To determine the *in vitro* efficacy of the new inhibitors, a dose response study was conducted to determine the IC_{50} values. On day three of incubation, the stock culture was dispersed as uniform 5 mL aliquots into sterile culture flasks, and the flasks were treated with test inhibitors in DMSO at 16 different concentrations from 1 to 100 µM and DMSO concentration was kept constant at 1% in all flasks. Following a 24 hours incubation, parasite viability was determined by the MTT assay. The data are plotted with a graphing software, GraphPad Prism 7.03 (GraphPad Software, San Diego, CA, USA). The software was used to calculate the IC_{50} values by fitting the data with a nonlinear regression with variable concentration, and the IC_{50} values are reported with 95% confidence interval.

Multiple dose study

The effect of two smaller doses in comparison to a single dose was evaluated by two sequential dosing of 50 µM inhibitor during log phase of growth at culture days 3 and 4 compared to one single dose of 100 µM at day 3. MTT assays were performed every 24 hours on all cultures starting on the first day of incubation and ending on the fifth day of incubation. The growth curves were plotted for each of the treatment groups.

Time of addition

A time of addition test was carried out by treating *L. tarentolae* promastigotes with 100 µM of each inhibitory compound at separate days in their growth curves to assess differing susceptibilities of cells at separate stages. New parasite cultures (10 mL per flask) were prepared, and they were grown for 7 consecutive days for the study. MTT analysis on each sample with or without additions was carried out the day after addition and each day thereafter. All the experiments were completed in parallel using the same cell stock, and the viability of each treated sample was normalized against the control cell culture (DMSO addition only).

Cell rescue assay using folic acid

To assess the effect that the addition of folate has on the efficacy of the three inhibitory compounds, cell cultures were prepared as previously described. In some flasks, 100 µM of inhibitor, or 100 µM folate, or 100 µM of inhibitor and 100 µM folate were added on the third day of incubation corresponding to the early logarithmic growth phase. In all cases, solutes were dissolved in DMSO and final DMSO concentration was 1%. Following 24 hours incubation, MTT assays were carried out on the cell cultures. These treatment groups were compared to cells that had only the inhibitors added on the third day.

Statistics

All statistical analyses were done with the software GraphPad Prism 7.03. The unpaired *t*-tests and one-way ANOVAs were employed to assess statistical significance, and a *p*-value of 0.05 was used as the threshold for statistical significance.

Results

Synthesis and spectroscopic characterization

The compounds of interest were synthesized by the reaction of 1-naphthalenesulfonyl chloride with the appropriate substituted aniline or phenol in the presence of base. Compound **A** was prepared as previously reported.[18] Compound **B** was prepared by refluxing the reactants in pyridine for 30 minutes followed by aqueous work up. Compound **C** was prepared by slow addition of an aqueous solution of the sodium phenoxide to the sulfonyl chloride in acetone, followed by aqueous work up. Compounds **B** and **C** were isolated in approximately 65% and 88% yields, respectively, while compound **A** was prepared in 47% yield as previously reported.

Both compounds **B** and **C** display ^{1}H NMR spectra that are in agreement with their structures. All three compounds were characterized by ESI-HRMS in 50:50 methanol:0.1% formic acid solution. For all three compounds, the most intense peak in the mass spectrum was the $[M+Na]^+$ ion (m/z = 364.0620 for **A**, m/z = 340.0152 for **B**, and m/z = 365.0444 for **C**) followed by the $[M+H]^+$ and $[M+K]^+$ peaks. Interestingly, even for compound **B**,

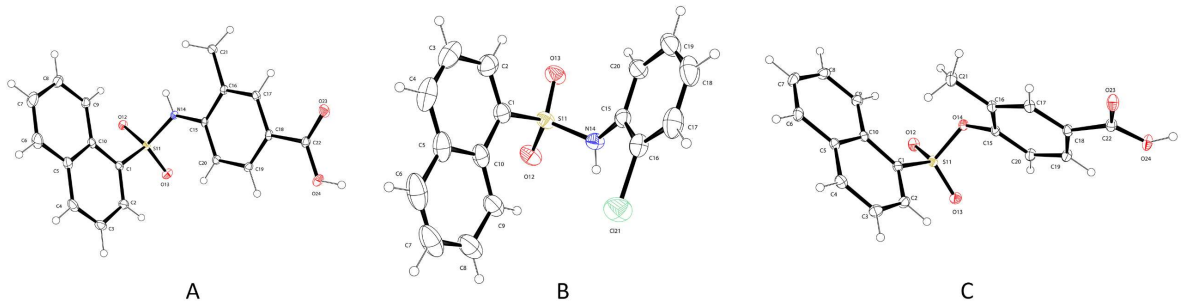

A B C

Figure 2. ORTEP diagrams for compounds **A**, **B**, and **C**. Displacement ellipsoids are drawn at the 50% probability level. Hydrogen atoms are drawn as spheres of arbitrary size.

which lacks a carboxylic acid group, the most intense peak was the sodium cation adduct, showing that the sulfonyl oxygens carry significant negative charges.

Crystal structure analysis

Single crystals of all three compounds were grown and subjected to single-crystal X-ray diffraction studies. The crystal refinement parameters are given in **Table S1** and bond distances and angles for the compounds are given in **Table S2**.

Compound **A** (**Figure 2A**) crystallizes in the monoclinic space group *C*2/*c* with *Z* = 4. All bond lengths and angles are in within the normal range for other sulphonamides (**Table S2**).[26] In compound **A**, the angle between the naphthalene and phenyl rings is nearly perpendicular at 88.58(4)° and the C1–S11–N14–C15 torsion angle is 65.53(12)°. In the crystal, compound **A** forms infinite chains via $R_2^2(8)$ carboxylate dimers and $R_2^2(8)$ sulfonamide dimers (**Figure 3**, **Table S3**). The hydrogen atom of the carboxylic acid group is disordered over both possible positions, but the structure was modelled without the disorder. The chains are linked together into a 3-dimensional network through C–H···O hydrogen bonds.

Compound **B** crystallizes in the monoclinic space group $P2_1/n$ with four molecules in the unit cell (**Figure 2B**). All of the bond length and angles are in the normal ranges for sulfonamide molecules (**Table S2**).[26] The angle between the phenyl and naphthalene rings in compound **B** is 71.88(5)° with a C1–S11–N14–C15 torsion angle of 56.54(14)°, both of which are smaller than in compound **A**. In the crystal lattice, the molecules form infinite *C*(4) chains through N–H···O hydrogen bonds (**Table S3**, **Figure 4a**) running along the *b*-axis. These chains form infinite 2-dimensional sheets via C–H···O hydrogen bonds (**Figure 4b**).

Compound **C**, the only sulfonate ester in the present study, crystallizes in the triclinic space group $P\bar{1}$ with *Z* = 2 (**Figure 2C**). As with the previous molecules, all of the bond lengths and angles (**Table S2**) in **C** are within range for similar compounds.[26] The angle between the naphthalene and phenyl rings in **C** is 63.84(5)°, significantly smaller than the angle in either **A** or **B**. The C1–S11–O14–C15 torsion angle is 71.86(12)°, which is larger than the analogous torsion angle in compounds **A** and **B**. In the crystal, molecules of **C** form dimers via the common $R_2^2(8)$ carboxylate hydrogen-bonding motif (**Table S3**, **Figure 5a**). These dimers form into ribbons via C–H···O hydrogen bonds formed between aromatic C–H and the terminal sulfonyl oxygen atom (**Figure 5b**).

Crystal structure comparison

Figure 6 shows stick diagram overlays of the molecules to visualize their conformational differences.[27] **Figure 6a** shows

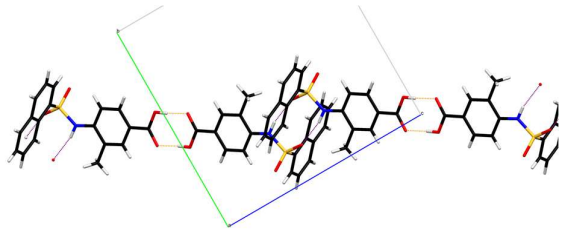

Figure 3. Hydrogen bonding network in compound **A**, showing carboxylate and sulfonamide dimer chains. Sulfonamide H-bonding interactions are shown in purple and carboxylic acid H-bonding interactions are shown in orange.

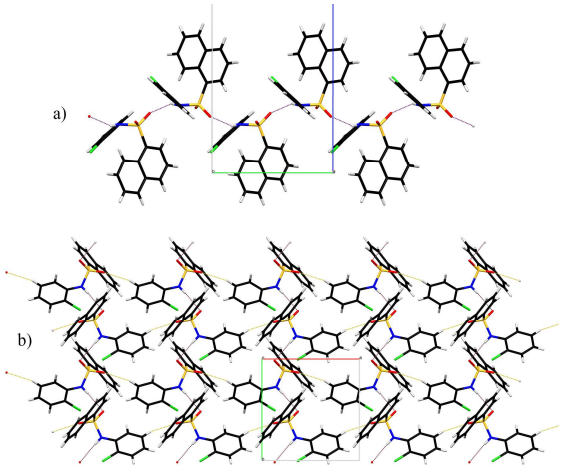

Figure 4. Hydrogen bonding networks in compound **B**, showing (top, a) sulfonamide *C*(4) chains and (bottom, b) the 3-dimensional network formed via C–H···O hydrogen bonds. Sulfonamide H-bonding interactions are shown in purple and C–H···O interactions are shown in orange.

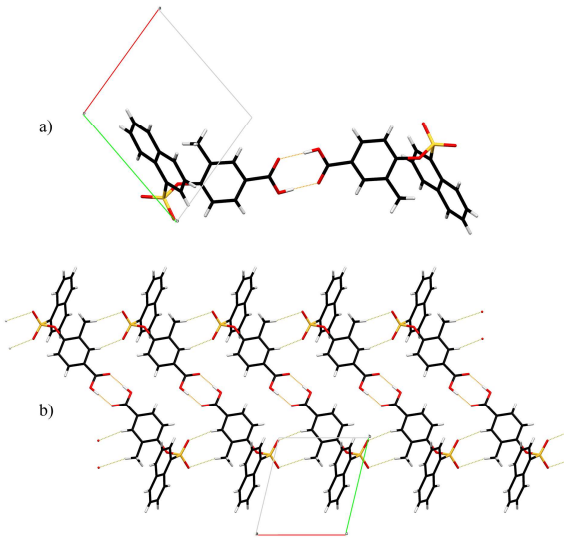

Figure 5. Hydrogen bonding networks in compound **C**, showing (top, a) the carboxylate dimer and (bottom, b) the 2-dimensional sheets formed via C–H···O hydrogen bonds. Carboxylic acid H-bonding interactions are shown in orange, and C–H···O interactions are shown in dark green.

overlay of the two carboxylate compounds **A** and **C** which only differ at atom 14 (an NH group in **A** and an oxygen atom in **C**). Looking at the bond length data in **Table 2**, the S–N bond in **A** [1.6316(13)Å] is about 0.03Å shorter than the analogous S–O bond in **C** [1.6021(12)Å]. Additionally, the S–N–C angle in **A** [125.97(10)°] is approximately 4.5° larger than the corresponding S–O–C angle in **C** [121.47(10)°]. As a result, the phenyl ring is swung further away from the naphthalene ring in compound **C** as compared to compound **A** (**Figure 6a**). The longer S–Z (Z = O or NH) distance along with the lack of steric interference between the *ortho*-methyl group and the sulfonamide hydrogen, H14, allows the phenyl group in compound **C** more freedom to rotate leading to a structure that is less compact than in compound **A**.

The sulfonamide compounds **A** and **B** (**Figure 6**) have similar conformations. The S–N bond lengths are very similar [1.6316(13)Å versus 1.6382(15)Å], but the S–N–C bond angle in **B** is significantly smaller than the analogous angle in **A** [125.97(10)° in **A**, 124.13(12)° in **B**]. This is due to the increased pyramidalization of the nitrogen in **B** as compared to **A**. In **B**,

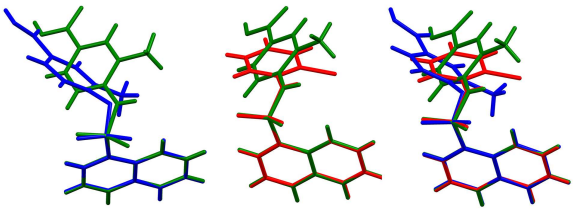

Figure 6. Structure overlays for compounds **A** (green), **B** (red), and **C** (blue).

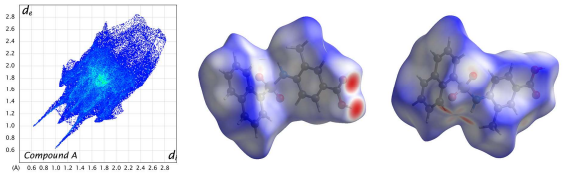

Figure 7. Fingerprint plot and two views of the Hirshfeld surface for compound **A**.

N14 sits 0.166Å above the plane defined by S11/H14/C15, while N14 sits only 0.122Å above the same plane in **A**; the increase in pyramidalization leads to smaller bond angles. The difference in the degree of pyramidalization between the two molecules is likely due to the electronic differences between the substituents on the phenyl rings in the two compounds. **Figure 6** also shows an overlay of all three compounds.

Hirshfeld analysis

All three structures were analysed using CrystalMaker.[28] **Figure 7** shows the fingerprint plot and Hirshfeld surface mapped over d_{norm} for compound **A**. Looking more closely at the interactions in **A**, the most common interactions are H···H interactions (35.6%), followed by O···H/H···O (27.7%), and C···H/H···C (24.7%). The strongest interactions, seen as spikes in the fingerprint plots, are the O···H/H···O interactions. The carboxylate and sulfonamide hydrogen-bonding interactions are seen as the red areas in the Hirshfeld surface plot for compound **A**, with the stronger carboxylate interactions showing up as larger, deeper red spots than the sulfonamide interactions.

Figure 8 shows the fingerprint plot and Hirshfeld surface for compound **B**. The first different to note between compounds **B** and **A**, are that the hydrogen-bond spikes in the fingerprint plot for **B** are shorter and wider than the spikes in the plot for **A**. This is due to the lack of a carboxylic acid group in compound **B**, which only has N–H···O hydrogen bonds from the sulfonamide group, which are generally weaker than the N–H···O hydrogen bonds of carboxylic acid groups. The major interactions in **B** are H···H (33.4%), C···H/H···C (26.2%), H···O/O···H (18.1%), and H···Cl/Cl···H (11.5%) interactions. The decrease in the occurrence of H…O/O…H interactions in **B** compared to compounds **A** and **C** is mainly due to the lack of the carboxylic acid group. In the Hirshfeld surface plot for **B**, the strongest interactions, indicated by larger red areas on the surface, are located near the sulfonamide hydrogen and oxygen atoms involved in the N–

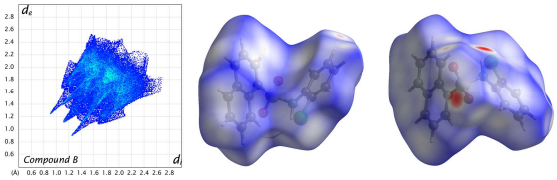

Figure 8. Fingerprint plot and two views of the Hirshfeld surface for compound **B**.

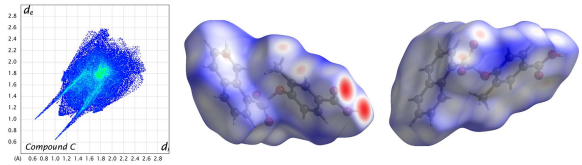

Figure 9. Fingerprint plot and two views of the Hirshfeld surface for compound **C**.

H···O hydrogen bonding. Additionally, there is a small area of red near H19, which is involved in C–H···O hydrogen bonding to link the chains into the two-dimensional sheets in the crystal structure.

The fingerprint plot and Hirshfeld surface for compound **C** are shown in **Figure 9**. The hydrogen bond spikes in the fingerprint plot of **C** are narrower at the base then those in the fingerprint plot of **A** due to the lack of N–H···O hydrogen bonds in the sulfonate ester. Otherwise, the overall shape for the fingerprint plot of **C** is very similar to that of **A**. The important interactions in **C** are H···H (38.8%), H···O/O···H (31.2 %), and H···C/C···H (16.6%) interactions. The Hirshfeld surface plot for compound **C** shows large red areas corresponding to the carboxylate hydrogen bonding interactions. Also, smaller red areas are seen near the terminal sulfonate oxygen atoms and H17 and H21C, which correspond to the C–H···O hydrogen bonds the link sulfonate ester dimers into ribbons in the crystal.

Comparing the three structures, H···H interactions are the predominant interactions, ranging from 33.4% to 38.7% of the intermolecular interactions in the crystals **(Figure S1)**. Interestingly, the H···O/O···H interactions have the greatest amount of variability between the three compounds. Compound **B** has the lowest amount of H···O/O···H interactions at 18.1%, while compound **C** has the largest, at 31.2%. It is somewhat interesting that the H···O/O···H interactions of **C** make up a larger percentage of the overall intermolecular interactions than in compound **A**, given that **A** has an additional hydrogen-bond donor group (N–H). However, the more open nature of

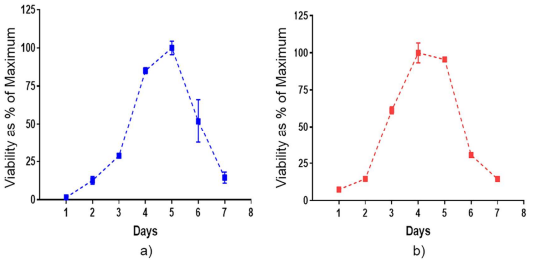

Figure 10. *L. tarentolae* promastigote growth curves *in vitro* at differing initial inoculation cell concentrations. a) low initial cell volume inoculation; b) Two-times higher initial cell volume inoculation.

the C–SO_2–O–C moiety in **C** compared to the C–SO_2–NH–C moiety in **A** allows greater hydrogen-bonding access to terminal sulfonyl oxygen atoms for C–H···O hydrogen bonds. None of the compounds display significant π-stacking between naphthalene or benzene rings, as evidenced by the low percentage of C···C contacts in the Hirshfeld surface analyses (**A**: 6.3%, **B**: 6.2%; **C**: 8.1%).

Evaluation of inhibitory effects on *L. tarentolae*

Growth Curve. Typical growth curves for *L. tarentolae* are shown in **Figure 10** and indicate that a difference in the initial number of cells used shifts the growth curve. Therefore, all experiments using test compounds were compared to control cells from the same original stocks so that cell number and viability were controlled. It is clear that the cells on days 0 to 2, days 2 to 4, day 5, and days 6 to 7 are in the lag phase, log phase, stationary phase and senescence phase, respectively, for cells grown from a low initial volume inoculation. Two days after a 100 µM addition of compound, compound **A** showed an 80% inhibition relative to the control cells while compounds **B** and **C** showed a 95% inhibition relative to control cells.

Dose Response and IC_{50}: Dose response of *L. tarentolae* in the logarithmic phase for each of the test compounds was assayed at 16 concentrations ranging from 1 µM to 100 µM (**Figure 11**).

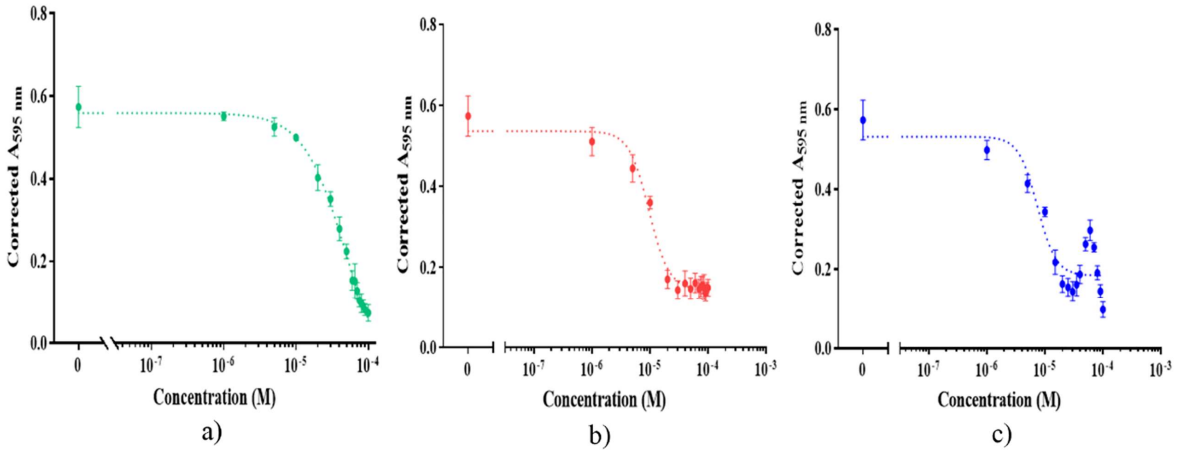

Figure 11. Dose response curves from 0-100 µM (16 concentrations, n = 4) in 1% DMSO after 24 hrs incubation. The points were fit in Graphpad Prism 7.03, and all IC_{50} values were reported with the 95% confidence interval: a) dose response curve for compound **A**; b) dose response curve for compound **B**; c) dose response curve for compound **C**.

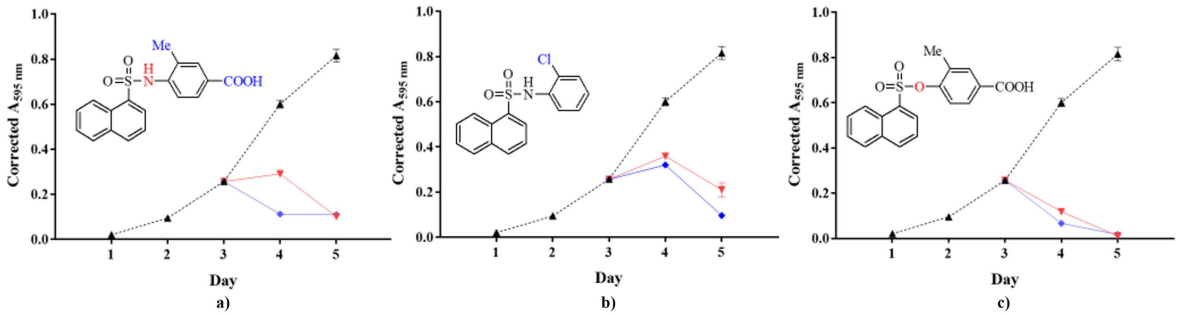

Figure 12. Dose accumulation study with compounds added on days 3 and 4 totalling 100 µM of compound compared to a single dose of 100 µM on day 3: a) compound **A**; b) compound **B**; c) compound **C**. The black triangles are 1% DMSO control, the blue diamonds are a single 100 µM addition on day 3, and the red triangles are 50 µM additions on each of day 3 and day 4.

The corrected responses were plotted as a function of concentrations, and IC_{50} values were determined within 95% confidence interval. The IC_{50} for the benchmark compound **A** was determined as 49 µM (**Figure 11a**). For the chloro-substituted sulfonamide **B**, the IC_{50} was determined to be 9.5 µM, which is 5 times lower than that of benchmark compound **A** (**Figure 11b**). Treatment with the sulfonate ester, **C**, provided an IC_{50} of 7.4 µM (**Figure 11c**). Interestingly, the sulfonate ester **C** appears to reach a local maximum of inhibition between 20 and 40 µM where it inhibits cell viability at 75%. However, as the concentration of this compound was increased, inhibition decreased until 55 – 65 µM of the compound only inhibited about 50% of parasite viability. Then, as concentration was increased to 100 µM, inhibition increased to 85% reduction in cell viability. This non-typical dose response is highly unusual but has been reported by others for endocrine disruptors.[29,30] The range of concentrations where **B** reaches 75% inhibition coincides with when it begins crystalizing; we observed noticeable crystallization *in vitro* in concentrations above 30 µM. The poor solubility may negatively affect its efficacy at higher concentration. Nevertheless, **B** is much more inhibitory than benchmark compound **A**, despite the poor solubility. Both compounds **B** and **C** have IC_{50} values in the range reported by Taylor *et al.*[31] of the EC_{50} value for amphotericin B effectiveness against axenic *Leishmania amazonensis* which was 9.2 ± 2.1 µM.

Dose Accumulation Study: To determine the effect of dose accumulation, the dose additive study was started during the cell logarithmic phase with a relatively lower cell concentration culture. One 50 µM dose of compound or DMSO on day 3 of the cell growth (**Figure 12**) was followed by an equal second dose (50 µM) on day 4; this was compared to one single dose of 100 µM on day 3 (**Figure 12**). Results show that on day 5 the sulfonate ester **C** and benchmark **A** are dose additive relative to the single 100 µM dose. Remarkably, after the first 50 µM dose the novel sulfonate ester effectively inhibits the cell growth comparable to the effectiveness of 100 µM one dose of the same compound, and both reached the lowest cell viability (**Figure 13**, III, 98-99%, $p < 0.05$) after 5 days. Surprising, chlorosulfonamide **B** reveals a different pattern with less reduction in cell viability 24 hours after the 100 µM treatment, as well as after the first 50 µM treatment. This delayed inhibition, compared to compounds **A** and **C**, one day after treatment with 100 µM of the compound could be related to the lower water solubility of compound **B**. As previously observed for the dose response study with chlorosulfonamide **B**, crystals appeared after the first dose and persisted after the second dose, similar to the 100 µM dose test. We suspect the poor solubility may negatively affect the cellular uptake and effectiveness of sulfonamide **B**.

Time of addition: The time of addition study is designed to evaluate inhibitory effectiveness for compounds **A**, **B**, and **C**

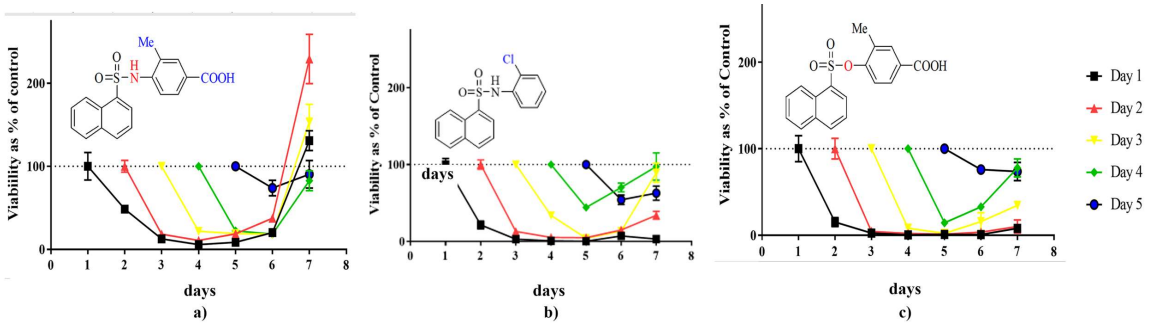

Figure 13. Effect of time of addition for inhibitory compounds at 100 µM: a) compound **A**; b) compound **B**; c) compound **C**.

additions at different times or phases during the cell culture cycle from day one (lag phase) to day five (stationary phase) at 100 µM. For control tests, 1% DMSO was added on any of the first five days of incubations and in all the tests, the DMSO did not affect any statistically significant change in parasite viability ($p < 0.05$, data not shown). The data were plotted as percent of control viability as a function of incubation time in days (**Figure 13**). Overall, the novel chlorosulfonamide **B** and sulfonate ester lead to cell inhibition significantly better than the benchmark compound, sulfonamide **A**.

Cells in early log phase appeared to be more sensitive to inhibition by all three compounds than cells in senescence. However, cells treated in log phase with Compound A appeared to have a late stage recovery in cell viability.

Effects of Folic Acid Addition: *Leishmania* are known to be auxotrophic for folate and pterin, relying on their mammalian hosts to supply these essential cofactors.[11,32] Sulfonamides are known competitive inhibitors for enzymes that utilize PABA to synthesize 7,8-dihydrofolate from pterin, which is further metabolized to tetrahydrofolate.[33] Tetrahydrofolate is an important one-carbon (1C) donor and acceptor in the 1C-metabolic pathway and is essential in the biosynthesis of thymidine and purines. We hypothesized that our novel sulfonamides may also be inhibiting these enzymes, and we proposed that if the addition of folic acid rescues cells from inhibition by these molecules we bypass the requirement for pterin metabolism for dihydrofolate production. Based on the relative cell viability assay, folate addition to the control cells increased growth by 13% (**Figure 14**). However, folate addition to cells with test compounds only modestly protects the cells from the inhibitory effects of compounds **A**, **B**, and **C** which alone inhibit 80, 70 and 90%, respectively. This suggests that these compounds are not strong folate pathway antagonists and other mechanisms are involved.

Discussion

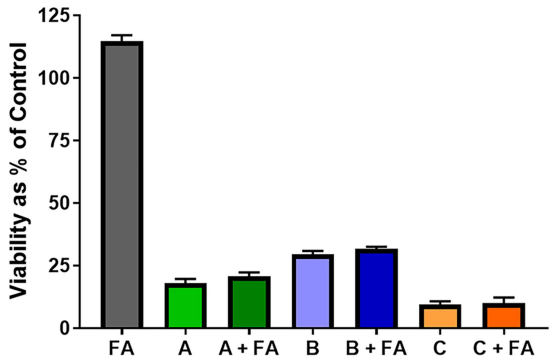

Figure 14. Effects of folate addition on cell viability 24 hours after addition of 100 µM folic acid (FA), or 100 µM test compound **A**, **B**, or **C**, or simultaneous addition of 100 µM folic acid and 100 µM test compound to cell cultures. Data are the mean ± SD for n=4 replicates.

Table 1. Comparison of IC_{50} values (µM) of the studied compounds and reference compounds.

Compound	IC_{50} value (µM)	reference	species studied
A	49	this work	*L. tarentolae*
B	9.5	this work	*L. tarentolae*
C	7.4	this work	*L. tarentolae*
amphotericin B	9.2 (EC_{50})	31	*L. amazonesis*
miltefosine	31.4	16	*L. amazonesis*
NiQNBS[a]	27	16	*L. amazonesis*

[a]*N*-isoquinolin-1-yl-4-nitrobenzenesulfonamide

With all three compounds tested in this study, a single 100 µM dose substantially reduced *in vitro Leishmania tarentolae* viability as shown in **Table 1**. The IC_{50} values reported for our novel sulfonamide compounds and sulfonate ester compound are substantially lower than those reported by Peixoto and Beverley[11] for different sulfonamide and sulfone compounds which were in the range of 150 µM or higher. The new compounds tested here thus have good anti-*Leishmania* properties, especially for compounds **B** and **C** from which the parasites do not appear to easily recover (as shown in **Figure 14).** This is especially true when the compounds are given in the early log phase of *in vitro* cell growth. Based on IC_{50} values, *L. tarentolae* promastigotes are much more sensitive to the newly synthesized chlorosulfonamide **B** and sulfonate ester **C** than to our benchmark sulfonamide **A**; the IC_{50} values of the novel molecules are at least 5 times lower than the benchmark **A** compound.

Interestingly, the dose response curve of compound **C** does not follow the classical shape that is usually observed in most dose response curves, including compounds **A** and **B** (**Figure 11c**). Essentially, this means that slope of the dose response plot changes sign at least once in the tested concentration range.[29] In this instance, the curve changes slope in two places; increasing at 20-25 µM and decreasing at 60-65 µM. Consequently, 20 µM of **C** is more toxic to the parasites than double or even triple that concentration. This unusual (non-monotonic) dose response relationship has been previously reported for other compounds but there is no universal mechanism that explains these results.[30] We speculate that in the intermediate concentrations, the parasites detect the toxic compounds and have some as yet unknown compensatory response(s). At the lower end (1-20 µM) of the scale, the concentration may not be high enough to trigger the compensatory response. At the higher end, the concentration may overwhelm the parasites' compensation efforts. Although we have no indication that the sulfonate ester behaves as an electrophile, future work will involve testing whether this is important in the mechanism(s) of cell viability inhibition. Further investigation is necessary to better understand this mechanism and determine ways to improve the molecule to resist this cellular response.

Since compounds **B** and **C** have comparable negative effects on *L. tarentolae in vitro*, but the chlorinated compound (**B**) is likely limited by its observed lower solubility at concentrations above 30 µM, we speculate that compound **B** could be even more

inhibitory than shown in these experiments. Indeed, we saw that in the dose response, time of addition, and folate effects studies, the effect of compound **B** as concentration increased from 50 μM to 100 μM did not increase as expected. Additionally, **B** appears unable to induce more than ~95% inhibition at any concentration after 24 hrs unlike the other two compounds, which could also be attributed to a solubility issue. After 48 hours, the inhibitory effect of **B** increases, apparently overcoming its solubility problem. We speculate that this is due to the continuous dissolution of the crystalized compound as the aqueous phase molecule interacts with the parasites. When two days or more incubation is permitted, compound **B** cumulatively inhibits parasite viability more than compound **A** and comparably with compound **C**. Fortunately, at lower concentrations near its IC_{50}, **B** is a very good inhibitor, and it appears to be sufficiently soluble. To gain better access to the abilities of chlorosulfonamides, future work should focus on increasing their solubility which may include synthesizing derivatives that include an addition carboxyl or other hydrophilic group.[34]

Folic acid pathways are increasingly attractive targets for *Leishmania* therapies.[6,35] *Leishmania* may be auxotrophic for folate, however they can scavenge the molecule from its growth medium.[11,36] The data from our folate study indicate that the addition of folate along with our three inhibitors does not protect the parasites, which suggests a mechanism that may not involve substantial inhibition of one or more folate pathway enzymes. This is in agreement with Peixoto and Beverley,[11] who reported active sulfa drugs effects were not relieved by folate addition. Folate is produced in the parasites by two enzymes: dihydrofolate reductase (DHFR) and pteridine reductase 1 (PTR1).[36] To effectively inhibit the folate pathway, both enzymes must be inhibited. Other likely sulfonamide targets in *Leishmania* are reported to include inhibition of carbonic anhydrase[37] and disruption of cell proliferation by disruption of microtubule activity.[38]

Our additive study results indicated that for **A** and **C**, but not for **B**, two sequential doses, 24 hours apart, of 50 μM was equivalent to a single 100 μM dose, suggesting that the effects of the compounds are additive. This is a desirable trait for *in vivo* leishmanial treatments because multiple small doses over time generally cause fewer side effects than a single large dose.[39]

Our time-of-addition study allowed us to conclude that the parasites were consistently most vulnerable to the compounds in their lag and logarithmic phases, especially in the early logarithmic phase, which was day 2 in these experiments. Though we saw that day 2 additions were most effective for 24 hour inhibition periods, day 1 additions were most effective in the long term. However, those cells that were treated with a single dose of compound **A** early in their growth curve recovered considerably after several days. Neither compound **B** nor **C** treated cells exhibited noticeable recovery back to control cell levels indicating more complete viability inhibition of the parasites. Each compound tested was less effective when added in the stationary or senescence phase. This, coupled with the observation that the compounds were most effective in the early logarithmic phase, suggests interference with cell proliferation as a possible mechanism of inhibition. In the literature, parasite clumping, and shape change are identifiers for late stage *Leishmania* promastigotes (stationary and senescence phases) as nutrients are depleted and waste increases.[40] In the cells treated with the three compounds early in their growth curves in the time-of-addition study, we did not observe clumping several days after treatment, but we did see the parasites change shape to a more circular morphology, reflecting cell death.[18]

There is a five-fold improvement in IC_{50} values between **A** and **B** as shown in **Table 1**. It appears substitution of the methyl group by chlorine plays an important role in increasing the compound's inhibitory ability. Halogenation has been reported to improve the protein-binding ability of agonists through the formation of strong non-bonding interactions, including halogen bonds.[41,42] In the crystal structure of **B**, there are no significant Cl···Cl interactions, but Cl···H interactions *are* significant, accounting for 11.5% of the total intermolecular interactions. This may point to Cl···H interactions being important in the inhibitory mechanism for compound **B**. Synthesis and testing of F, Br, I and CF_3 substituted analogues would grant us insight into the structure-activity relationships of size and polarity. We can confidently infer that chloro- and perhaps other halogen sulfonamides or sulfonate esters are promising compounds for future SAR studies and inhibitory testing.

The IC_{50} value of the sulfonate ester **C** is also lower than that of sulfonamide **A**. We can attribute the significant improvement in inhibitory activity to the substitution of the NH for an oxygen. The substitution decreases the polarity and steric hindrance, potentially giving more chance for conformation adaption to a putative active site. In addition to decreasing polarity, the substitution changes the linking atom from a hydrogen-bond donor group to a potential hydrogen-bond acceptor group. Altering the linkage between the naphthalene and the benzene with and without halogen substitution on the benzene are of great interest to further evaluate the potency of the molecules as inhibitors of *Leishmania*.

Figure 15 presents a summary of our observations on the inhibitory ability of naphthalene sulfonyl compounds studied by us. First, substitution of in the *para*-position of the phenyl ring, Y, does not appear to significantly alter the potency of the molecules, but addition of a carboxylic acid group greatly enhances the water solubility. Next, the substituent at the X position (*ortho* on the phenyl ring), does appear to be important to function. Presence of larger groups, such as methoxy and thiomethyl, or a smaller hydrogen group, at the X position lowers the effectiveness of the sulfonamide molecules overall.[18] As shown in this and our previous study, compounds with chloro or methyl groups in the X position are good inhibitors of *Leishmania*. Additionally, placement of either an oxygen atom or an N–H group at position Z, linking the naphthene sulfonyl group and the aryl ring, appears to lead to molecules that are excellent inhibitors of *Leishmania*. Finally, unpublished results

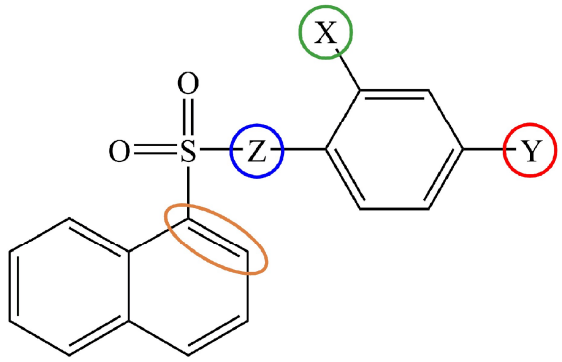

Figure 15. Generic structure of naphthalene sulfonyl compounds studied by our group, with important areas of substitution highlighted. Our studies indicate that the position of substitution on the naphthalene ring (orange oval) and the size of the ortho substituent, X, are important for anti-leishmanial activity. The identity of the group in the *para*-position, Y, and the identity of the Z group (O or NH) does not affect the potency.

from our laboratories have shown that 2-naphthalene sulfonyl compounds are poor inhibitors of *Leishmania*.

Conclusions

We have demonstrated that the two newly synthesized novel molecules, naphthalene chlorosulfonamide **B** and sulfonate ester **C**, are potent inhibitory compounds against *Leishmania tarentolae* promastigotes *in vitro*. The high toxicity of the novel compounds **B** and **C** against *L. tarentolae* brings new perspective to structure-activity relationships that are beneficial for the treatment of leishmaniasis. We believe that continued SARs studies on halogen substituted sulfonamides and sulfonate esters is a fruitful direction to develop new therapies toward treating this disease.

Conflicts of interest

There are no conflicts to declare.

Acknowledgements

CGH wishes to thank Illinois State University (URG-FRA award) and we all thank the Illinois State University Chemistry Department for financial support. We also thank the NSF (Grant no. CHE-1039689) for funding the X-ray diffractometer.

References

1 M. Kindhauser, Global defence against the infectious disease threat, World Health Organization, 2002.
2 Global Health Observatory (GHO) data, Leishmaniasis. https://www.who.int/gho/neglected_diseases/leishmaniasis/en/, (accessed 6/23/2020).
3 S.L. Roth, N. Malani and F.D. Bushman, *J. Virol.* 2011, **85**, 7393–7401.
4 S.L. Croft, S. Sundar and A.H. Fairlamb, *Clin. Microbiol. Rev.* 2006, **19**, 111–126.
5 N.C. Hepburn, *Clin. Exp. Dermatol.* 2000, **25**, 363–70.
6 R. Pathak and S. Batra, *Anti-Infect. Agents Med. Chem.* 2009, **8**, 226–267.
7 P. Hotez, R. Gupta, R. Mahoney and G. Poste, *Rev. Panam. Salud. Publica* 2006, **19**, 118–23.
8 M.R. Dikhit, B. Purkait, R. Singh, B.R. Sahoo, A. Kumar, R.K. Kar, M.Y. Ansari, S. Saini, K. Abhishek, G.C. Sahoo, S. Das and P. Das, *Drug Des. Devel. Ther.* 2016, **10**, 1753–61.
9 J. Drews, *Science,* 2000, **287**, 1960–4.
10 D.A. Smith and R.M. Jones, *Curr. Opin. Drug Discov. Devel.*, 2008, **11**, 72–9.
11 M.P. Peixoto and S.M. Beverley, *Antimicrob. Agents Chemother.*, 1987, **31**, 1575–8.
12 R.K. Marra, A.M. Bernardino, T.A. Proux, K.S. Charret, M.L. Lira, H.C. Castro, A.M. Souza, C.D. Oliveira, J.C. Borges, C.R. Rodrigues, M.M. Canto-Cavalheiro, L.L. Leon and V.F. Amaral, *Molecules*, 2012, **17**, 12961–73.
13 C. Barea, A. Pabon, D. Castillo, M. Zimic, M. Quiliano, S. Galiano, S. Perez-Silanes, A. Monge, E. Deharo and I. Aldana, *Bioorg. Med. Chem. Lett.*, 2011, **21**, 4498–502.
14 M. Goodarzi, E.F. da Cunha, M.P. Freitas and T.C. Ramalho, *Eur. J. Med. Chem.*, 2010, **45**, 4879–89.
15 K.M. Khan, M.Z. Khan, M. Taha, G.M. Maharvi, Z.S. Saify, S. Parveen and M.I. Choudhary, *Nat. Prod. Res.*, 2009, **23**, 479–84.
16 C. Galiana-Roselló, P. Bilbao-Ramos, M.A. Dea-Ayuela, M. Rolón, C. Vega, F. Bolás-Fernández, E. García-España, J. Alfonso, C. Coronel and M.E. González-Rosende, *J. Med. Chem.*, 2013, **56**, 8984–98.
17 K.K. Manar, C.L. Yadav, N. Tiwari, R.K. Singh, A. Kumar, M.G.B. Drew and N. Singh, *CrystEngComm*, 2017, **19**, 2660-72.
18 J. Katinas, R. Epplin, C. Hamaker and M.A. Jones, *Anti-Infect. Agents*, 2017, **15**, 57–62.
19 V.M. Taylor, D.L. Muñoz, D.L. Cedeño, I.D. Vélez, M.A. Jones and S.M. Robledo, *Exp. Parasit.* 2010, **126**, 471-475.
20 Enraf-Nonius, CAD4 Express Software, Delft, The Netherlands, 1994.
21 K. Harms and S. Wocadlo, XCAD-4: Program for Processing CAD-4 Diffractometer Data, University of Marburg, Germany, 1995.
22 A.C.T North, D.C. Phillips and F.S. Mathews, *Acta Cryst.*, 1968, **A24**, 351–359.
23 G.M. Sheldrick, *Acta Cryst.*, 2015, **A71**, 3–8.
24 J.B. Morgenthaler, S.J. Peters, D.L. Cedeno, M.H. Constantino, K.A. Edwards, E.M. Kamowski, J.C. Passini, B.E. Butkus, A.M. Young, T.D. Lash and M.A. Jones, *Bioorg. Med. Chem.*, 2008, **16**, 7033–8.
25 T. Mosmann, *J. Immunol. Methods*, 1983, **65**, 55–63.
26 C.R. Groom, I.J. Bruno, M.P. Lightfoot and S.C. Ward, *Acta Cryst.*, 2016, **B72**, 171–179.
27 C.F. Macrae, I.J. Bruno, J.A. Chisholm, P.R. Edgington, P. McCabe, E. Pidcock, L. Rodriguez-Monge, R. Taylor, J. van de Streek and P.A. Wood, *J. Appl. Cryst.*, 2008, **41**, 466–470.
28 M.J. Turner, J.J. McKinnon, S.K. Wolff, D.J. Grimwood, P.R. Spackman, D. Jayatilaka and M.A. Spackman, CrystalExplorer 17.5, University of Western Australia, 2017.
29 F. Lagarde, C. Beausoleil, S.M. Belcher, L.P. Belzunces, C. Emond, M. Guerbet and C. Rousselle, *Environ. Health*, 2015, **14**, 13.
30 L.N. Vandenberg, T. Colborn, T.B. Hayes, J.J. Heindel, D.R. Jacobs Jr., D.H. Lee, T. Shioda, A.M. Soto, F.S. vom Saal, W.V. Welshons, R.T. Zoeller and J.P. Myers, *Endocr. Rev.*, 2012, **33**, 378–455.
31 V.M. Taylor, D.L. Cedeño, D.L. Muñoz, M.A. Jones, T.D. Lash, A.M. Young, M.H. Constantino, N. Esposito, I.D. Vélez and S.M. Robledo, *Antimicrob. Agents Chemother.*, 2011, **55**, 1-10.

32 A. El Fadili, C. Kundig, G. Roy and M. Ouellette, *J. Biol. Chem.*, 2004, **279**, 18575–82.
33 A. Bermingham and J.P. Derrick, *BioEssays*, 2002, **24**, 637–648.
34 K.T. Savjani, A.K. Gajjar and J.K. Savjani, *ISRN Pharm.,* 2012, **2012**, 195727.
35 F. Zuccotto, A.C. Martin, R.A. Laskowski, J.M. Thornton and I.H. Gilbert, *J. Comput. Aided Mol. Des.*, 1998, **12**, 241–57.
36 T.J. Vickers and S.M. Beverley, *Essays Biochem.*, 2011, **51**, 63–80.
37 C.T. Supuran, F. Briganti, S. Tilli, W.R. Chegwidden and A. Scozzafava, *Bioorg. Med. Chem.*, 2001, **9**, 703–714.
38 Z. Liu, W. Tian, S. Wang, X. Luo, and Q. Yu, *Acta Pharmacol. Sin.*, 2012, **33**, 261–270.
39 E.A. Khalil, T. Weldegebreal, B.M. Younis, R. Omollo, A.M. Musa, W. Hailu, A.A. Abuzaid, T.P.C. Dorlo, Z. Hurissa, S. Yifru, W. Haleke, P.G. Smith, S. Ellis, M. Balasegaram, M., A.M. El-Hassan, G.J. Schoone, M. Wasunna, R. Kimutai, T. Edwards and A. Hailu, *PLoS Negl. Trop. Dis.*, 2014, **8**, e2613.
40 A.T. Christensen, C.C. McLauchlan, A. Dolbecq, P. Mialane and M.A. Jones, *Oxid. Med. Cell. Longev.,* 2016, **2016**, 9025627.
41 G. Gerebtzoff, X. Li-Blatter, H. Fischer, A. Frentzel and A. Seelig, *ChemBioChem*, 2004, **5**, 676–84.
42 M.Z. Hernandes, S.M. Cavalcanti, D.R. Moreira, W.F. de Azevedo Jr. and A.C. Leite, *Curr. Drug Targets*, 2010, **11**, 303–14.